Available online at www.sciencedirect.com

SCIENCE DIRECT®

Biochemical and Biophysical Research Communications 334 (2005) 86–95

BBRC

www.elsevier.com/locate/ybbrc

Gene expression profiling of the preclinical scrapie-infected hippocampus

Alan R. Brown [a], Selma Rebus [b], Clive S. McKimmie [a], Kevin Robertson [c], Alun Williams [b,1], John K. Fazakerley [a,*]

[a] Centre for Infectious Diseases, University of Edinburgh, UK
[b] Institute of Comparative Medicine, Department of Veterinary Pathology, University of Glasgow, UK
[c] Scottish Centre for Genomic Technology and Informatics, University of Edinburgh, UK

Received 7 June 2005
Available online 23 June 2005

Abstract

The molecular events that underlie prion disease neuropathology remain poorly defined. Within the hippocampus of the ME7/CV mouse scrapie model, profound CA1 neuronal loss occurs between 160 and 180 days post-infection (dpi). To elucidate the molecular events that may contribute to this neuronal loss, we have applied Affymetrix high-density oligonucleotide probe arrays to the study of ME7-infected hippocampal gene expression at 170 dpi. The study has identified 78 genes that are differentially expressed greater than 1.5-fold within the preclinical ME7-infected hippocampus prior to the profound late stage glial cell activation. The results indicate oxidative and endoplasmic reticulum (ER) stress, activated ER and mitochondrial apoptosis pathways, and activated cholesterol biosynthesis within the scrapie-infected hippocampus, and offer insight into the molecular events which underlie the neuropathology.

Keywords: Scrapie; Prion disease; Gene expression; Microarray; Endoplasmic reticulum stress; Apoptosis; Cholesterol; Neurodegeneration; Hippocampus

The transmissible spongiform encephalopathies (TSEs), or prion diseases, are a group of fatal, transmissible neurodegenerative diseases of humans and animals, including scrapie in sheep, bovine spongiform encephalopathy (BSE) in cattle, and Creutzfeldt–Jakob disease (CJD) in humans, that are typically characterized by the accumulation of a protease-resistant isoform (PrP^{Sc}) of the host-encoded prion protein (PrP^{C}) [1]. Whilst the major neuropathological features of these diseases are well documented (for review, see [2]), the host response to prion infection and the molecular events that underlie the TSE neuropathology are poorly defined. An understanding of these events is crucial to allow a focussed assessment of potential therapeutic targets.

Attempts to understand the molecular neuropathology of TSEs are particularly focussed on identifying host-encoded genes that are altered in expression as a consequence of the disease process. The majority of gene expression studies of TSE-infected brain have been performed at terminal stages of disease, and thus detect a predominance of glial-associated genes, reflecting the profound glial cell activation that is evident in the later stages [3]. Whilst there is evidence that glial cells and their products can influence the progression of TSE disease [4], it is also clear that several neuropathological features precede glial cell activation [5–7]. An understanding of the

* Corresponding author. Fax: +44 131 650 6511.
E-mail address: John.Fazakerley@ed.ac.uk (J.K. Fazakerley).
[1] Present address: Department of Pathology and Infectious Diseases, Royal Veterinary College, Hawkshead Lane, North Mymms, nr. Hatfield, Hertfordshire AL9 7TA, UK.

0006-291X/$ - see front matter
doi:10.1016/j.bbrc.2005.06.060

molecular events occurring at these earlier stages of disease, un-obscured by the profound glial cell activation, is essential to understand disease mechanisms. In a previous study, we applied Atlas expression arrays (BD Biosciences, Clontech) to the study of the molecular neuropathology of ME7 murine scrapie, identifying seven genes that were consistently upregulated at terminal disease (240 days post-infection, dpi) [8]. As anticipated, these genes were primarily glial cell-associated and included glial fibrillary acidic protein (GFAP) and vimentin. Analysis of the timecourse of upregulation by quantitative RT-PCR (QRT-PCR) found that the expression of all of these genes within the hippocampus was elevated from 170 dpi, a preclinical timepoint that coincides with a 20-day period (160–180 dpi) in the ME7/CV model during which 50% of the CA1 hippocampal neurons are lost [6]. It was considered unlikely that the upregulation of these genes had a direct role in the observed neuronal changes evident within the hippocampus at 170 dpi. To elucidate the molecular events that may contribute directly to the observed hippocampal neuronal loss, we have extended our studies of ME7-infected hippocampal gene expression at 170 dpi using the more comprehensive Affymetrix high-density oligonucleotide probe arrays. The study has identified 78 genes that are differentially expressed greater than 1.5-fold within the preclinical ME7-infected hippocampus at 170 dpi. The majority of these genes have not been reported before in the context of TSE neuropathology, and offer further insight into the molecular events that underlie the neuropathogenesis of prion disease.

Materials and methods

Animals. C57BLxVM/Dk mice (CV mice) were inoculated intracerebrally at 4–7 weeks of age with 20 μl of a 1% homogenate (in PBS) of a ME7-infected brain taken from a clinically affected C57BL mouse. Mice inoculated with 20 μl of a 1% normal brain homogenate (NBH) acted as controls. Recipient mice were killed at 40, 70, 100, 130, 160, 170, 180, and 210 dpi and at term (225–235 dpi). For genomic analysis, brains were perfused with DEPC-treated PBS prior to microdissecting the hippocampi free from the rest of the brain, using a stereotaxic microscope. Tissue was snap-frozen in liquid nitrogen for subsequent RNA extraction.

RNA preparation and microarray analysis. Total RNA was extracted from the hippocampus of three ME7-infected and three mock-infected CV mice (at 170 dpi) using the commercially available TRIzol reagent (Invitrogen) according to the manufacturer's instructions. Total RNA was treated with RQ1 RNase-free DNase (Promega), cleaned-up using an RNeasy Mini Kit (Qiagen), and analysed on an Agilent BioAnalyzer 2100 (Agilent Technologies) prior to microarray analysis. For microarray analysis, target RNA was prepared by converting 10 μg RNA into double-stranded cDNA (Superscript Choice System, Invitrogen) with a T7-$(dT)_{24}$ primer, which incorporates a T7 RNA polymerase promoter. Biotin-labelled cRNA was then synthesized from the cDNA using an RNA transcript labelling kit (Enzo Biochem). The biotin-labelled cRNA was fragmented prior to hybridization (16 h at 45 °C) to a Murine Genome U74Av2 array (Affymetrix, Santa Clara, CA). The Affymetrix MG-U74Av2 array represents all sequences (~6000) in the Mouse UniGene database (Build 74) that have been functionally characterized, in addition to ~6000 EST clusters. After hybridization, arrays were automatically washed and stained with streptavidin–phycoerythrin in an Affymetrix Fluidics Station 400, then scanned using an Agilent GeneChip 2500 Scanner, and the data were processed using the Microarray Analysis Suite v5.01 (MAS; Affymetrix). To enable comparison across the six arrays, all were scaled (using a global scaling method) to an overall target intensity of 100.

Microarray quality assurance. To ensure the quality and consistency of the sample labelling process and array hybridizations, control information from all six arrays was collated and reviewed prior to the data analysis. In brief, scaling factors (range 0.85–1.04), Raw Q values (range 2.16–3.29), GAPDH 3′/5′ ratios (range 0.81–1.0), and β-actin ratios (range 1.27–1.53) were all consistent with Affymetrix recommendations. To further investigate the performance of the array hybridizations, scatter plots comparing each array with every other were produced in SPLUS (Insightful, USA). These plots confirmed that the data had a symmetrical distribution and showed a dynamic uninterrupted range of expression values from low to high signal values. Box and whisker visualizations also confirmed that the data were symmetrical and of sufficient quality for further analysis (data not shown, experimental data and links to supplementary data can be obtained from the Scottish Centre for Genomic Technology and Informatics GPX database (www.gti.ed.ac.uk; experiment Accession No. GPX-000046.1). Full details of the study, including all experimental data, are also available at ArrayExpress (www.ebi.ac.uk/arrayexpress; experiment Accession No. E-MEXP-284).

Microarray data analysis. At the outset of the analysis, genes defined as 'absent' in all six replicates (by the MAS 5.01 algorithm) were removed from the dataset. Signal values for the remaining 6899 genes were then log (base 2) transformed in Excel (Microsoft, USA). For explorative analysis, genes were filtered on the basis of the coefficient of variance (CV = standard deviation of all six replicate signal values/mean of six replicate signal values). Briefly, CV and mean signal values (log base 2) were calculated for each gene and plotted against each other (data not shown). Variable genes (CV > 0.1) were selected for hierarchical clustering (using Pearson correlation as a distance measure) in GeneSpring (Silicon Genetics, USA) (Fig. 1). To identify notable gene expression changes in the filtered subset of 6899 genes, the open-source R based software 'Bioconductor' was used to implement a robust empirical Bayes 'moderated' t test using the log (base 2) transformed dataset [9].

Annotational information for differentially expressed genes was obtained from the Affymetrix resource 'NetAffx' (www.affymetrix.com/analysis), the Database for Annotation, Visualization, and Discovery v 2.0 (http://david.niaid.nih.gov/david/version2/index.htm), GeneCards (http://bioinfo.weizmann.ac.il/cards/index.shtml), and Genespring (Silicon Genetics, USA).

Real-time quantitative RT-PCR validation. The PowerScript Reverse Transcriptase system (Clontech) was used to synthesize cDNA from total RNA, prior to real-time PCR using the LightCycler Real-time PCR system as described previously [8]. Primer sequences are available upon request. Results were normalized for β-actin mRNA levels to ensure equivalence of the samples.

Results

Affymetrix MG-U74Av2 GeneChips were used to study gene expression in three ME7-infected and three control hippocampal samples at 170 dpi. Of the 12,488 genes and ESTs represented on the MG-U74Av2 array, approximately 55% had detectable expression in one or more of the samples studied. Hierarchical clustering of a

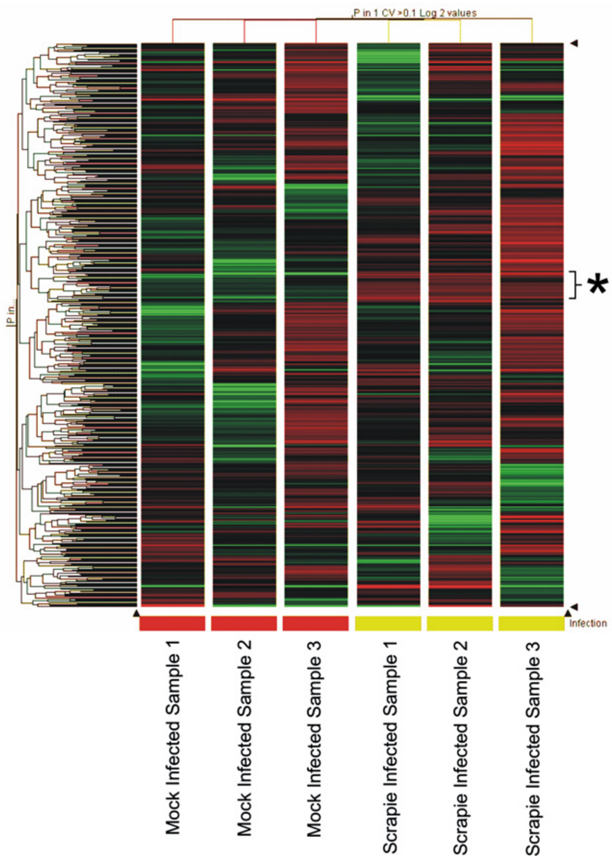

Fig. 1. Hierarchical clustering of replicate samples and differentially expressed genes. Data were pre-filtered on the basis of detection and 6899 genes were identified which had at least one replicate called as 'present.' Variable genes were then identified by filtering on the basis of the coefficient of variance as follows. Signal values were log transformed (log2) and a CV value was calculated (SD for all replicates/mean of all six replicates) for all replicates. Genes with CV value of >0.1 (568) were taken forward to hierarchical clustering (using Pearson correlation as a distance measure) in GeneSpring. Prior to clustering, the signal value for each gene was divided by the median of its measurements in all samples. If the median of the raw values was below 1 then each measurement for that gene was divided by 1 if the numerator was above 1, otherwise the measurement was thrown out. The image above shows clustering (of log2 values) on the basis of gene and group, and demonstrates a clear segregation of the replicate groups. To aid in visualization of the data, green represents a decrease in expression from the median value, whereas red represents an increase. (*) Cluster of genes with a comparable pattern of expression (see text).

variable subset of 568 genes resulted in the clear segregation of control and scrapie-infected samples (Fig. 1). It is notable that consistent patterns of differential gene expression were observed when control and scrapie-infected samples were compared. Furthermore, when the constituent members of the clusters were annotated, it was clear that the analysis had identified several genes of particular interest. For example, within the cluster identified with an asterisk, mediators of cholesterol biosynthesis (sterol-C4-methyl oxidase and sterol-C5-desaturase) and protein degradation (proteasome subunit, β type 5) were observed. To extend this analysis, the application of an empirical Bayes moderated *t* test identified 78 genes with a *p* value of less than 0.01 and a fold change of >1.5. Of these transcripts, 65 were upregulated and 13 downregulated more than 1.5-fold in the ME7-infected hippocampus samples relative to the uninfected controls. All notable genes ($p < 0.01$) with a fold change greater than 1.5 are listed in Fig. 2. Where possible, a functional classification has been assigned. It should be emphasized that the designation of functional class in the present study is not definitive, as annotation of gene function is incomplete, and multifunctional gene products can be involved in several cellular pathways.

To validate the array data, QRT-PCR analysis was performed on a selection of the differentially expressed genes (sterol-C4-methyl oxidase, sterol-C5-desaturase, complement component C1qβ, short coiled-coil protein, signal recognition particle 9, THUMP domain-containing 1, and neurofilament-L). All genes studied by QRT-PCR were confirmed as being differentially expressed within the 170 dpi hippocampus (data not shown). Three of these genes (neurofilament-L, sterol-C5-desaturase, and sterol-C4-methyl oxidase) were studied further by QRT-PCR, to examine the timecourse of differential expression between 170 dpi and terminal disease. In contrast to known glial cell-associated genes, which demonstrated increasing levels of expression through to terminal disease, the expression timecourse of neurofilament-L, sterol-C5-desaturase, and sterol-C4-methyl oxidase all showed decreased expression at terminal disease, despite an earlier increase (Fig. 3).

In contrast to comparable studies of late or terminal stage scrapie-infected brain [10,11], very few of the 65 upregulated genes identified in the present study were overtly immune-related or inflammatory. The upregulation of complement component C1qβ, TYRO protein tyrosine kinase (TYROBP or DAP12), and T-cell immunomodulatory protein are notable exceptions. DAP12, which is present on natural killer (NK) cells and myeloid cells, forms a receptor signalling complex in conjunction with TREM2 (triggering receptor expressed on myeloid cells 2b) [12]. Whilst only DAP12 was identified in the present study, both DAP12 and TREM2 have previously been shown to be upregulated in ME7-infected brain [11]. A recent study has demonstrated that the TREM2/DAP12 innate immune receptor complex enhances phagocytosis of apoptotic neurons and minimizes the proinflammatory microglial response [13]. Whilst the immune and inflammatory response within the 170 dpi hippocampus appears to be at a very early stage, the array data suggest an ongoing oxidative stress–response, with upregulation of both the antioxidant enzyme peroxiredoxin 2 and proteasome β5 subunit. The latter is known to have antioxidant response elements within its promoter [14]. Upregulation of erythroid differentiation regulator (edr1), an autocrine survival factor in-

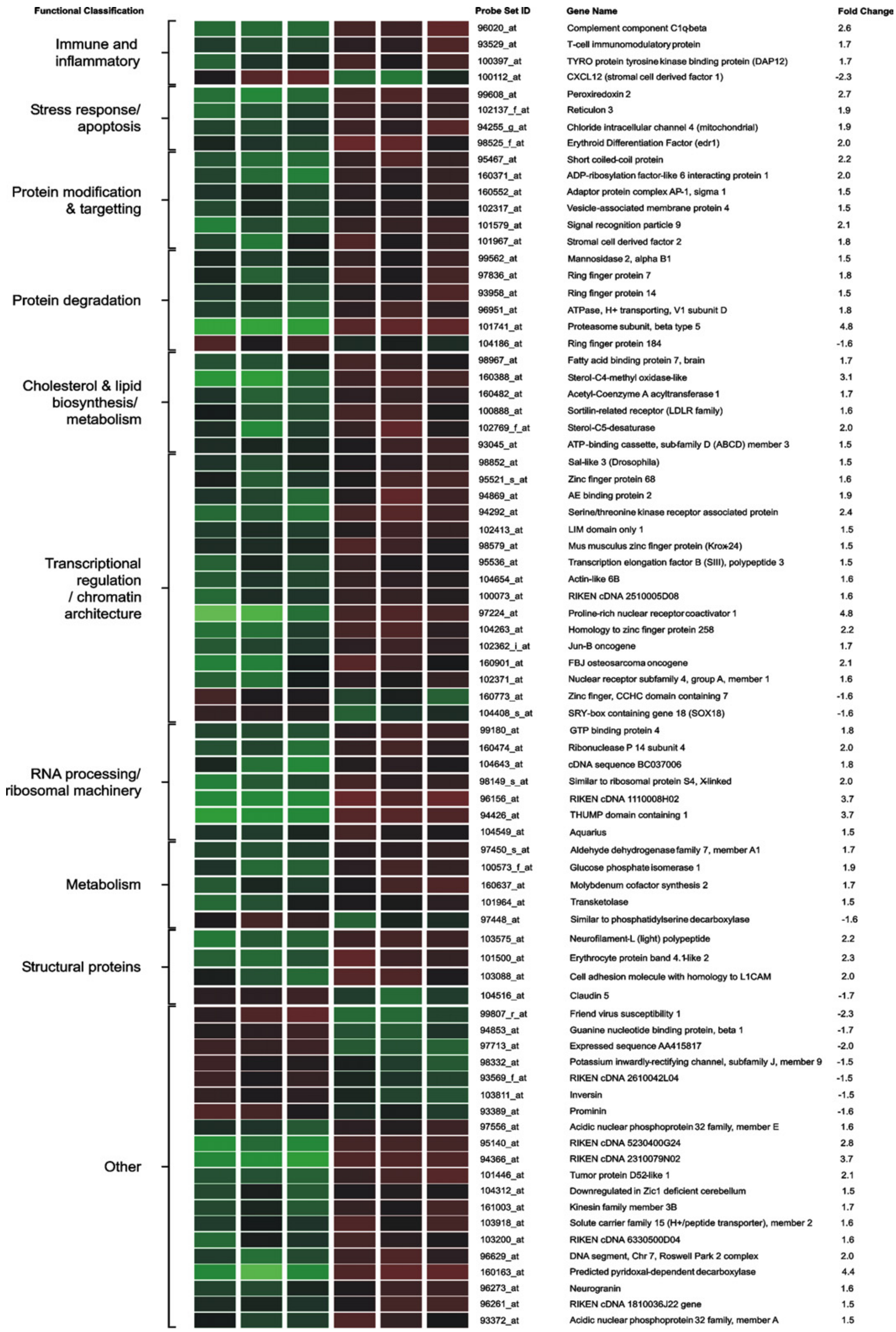

Fig. 2. Differentially expressed genes identified within the ME7-infected hippocampus. Data were pre-filtered on the basis of detection and 6899 genes were identified which had at least one replicate called as present. To identify notable gene expression changes in the filtered subset of 6899 genes, the open-source R based software 'Bioconductor' was used to implement a robust empirical Bayes 'moderated' t test using a log (base 2) transformed dataset [9]. The application of the empirical Bayes t test identified 78 genes with a p value of less than 0.01 and a fold change of >1.5. Of these transcripts, 65 were upregulated and 13 downregulated more than 1.5-fold in the ME7-infected hippocampus samples relative to the uninfected controls. Differentially expressed transcripts were annotated as described under Materials and methods. To generate the figure above, each gene was divided by the median of its measurements in all samples. If the median of the raw values was below 1 then each measurement for that gene was divided by 1 if the numerator was above 1, otherwise the measurement was thrown out. To aid in visualization of the data, green represents a decrease in expression from the median value, whereas red represents an increase.

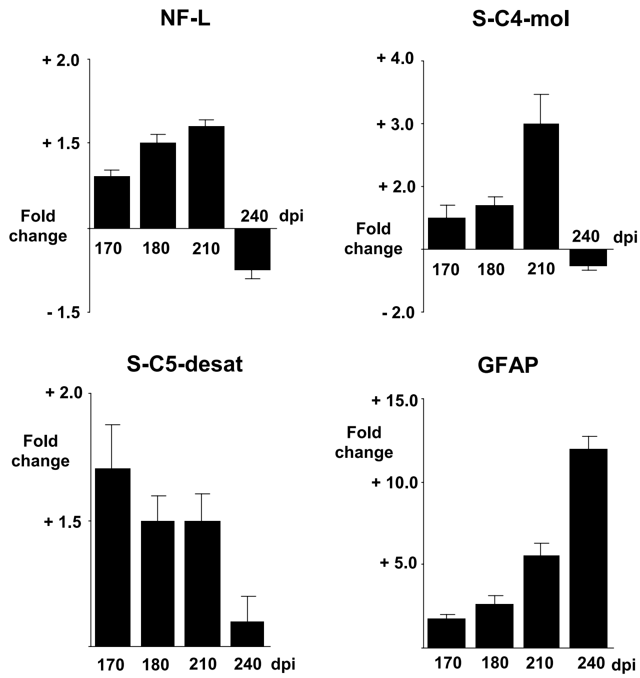

Fig. 3. Timecourse analysis of selected genes by quantitative RT-PCR. Expression of neurofilament-L (NF-L), sterol-C4-methyl oxidase (S-C4-mol), sterol-C5-desaturase (S-C5-desat), and GFAP was studied within the ME7-infected hippocampus between 170 dpi and terminal disease. Four control and four ME7-infected hippocampus samples were studied at each timepoint. Charts above show the mean fold change at each timepoint ± SEM. In each chart, the *Y*-axis intercept is equivalent to the control expression level (i.e., no change in the ME7-infected sample, relative to control).

duced by various stress conditions [15], provides further evidence of cellular stress.

Cellular stress is inextricably linked to perturbation of endoplasmic reticulum (ER) and mitochondrial homeostasis, and the array data suggest that the normal function of both of these cellular compartments is impaired within the scrapie-infected hippocampus. Reticulon 3, an ER-localized protein that can cause the rapid depletion of ER calcium stores, thus triggering apoptosis [16,17], was upregulated in the present study. Additionally, the present study provides evidence of an activated mitochondrial apoptotic pathway. Direct overexpression of the mitochondrial chloride channel mtCLIC4, which was upregulated in the ME7-infected hippocampus, has been shown to reduce the mitochondrial membrane potential, triggering the release of cytochrome *c* into the cytoplasm and initiating caspase-mediated apoptosis [18]. Further evidence of the activation of the mitochondrial apoptotic pathway is provided by the upregulation of ring finger protein 7 (also known as SAG, sensitive to apoptosis gene), HtrA2, and two members of the acidic nuclear phosphoprotein 32 family, Anp32A and Anp32E. SAG functions to inhibit or delay cytochrome *c* release and caspase activation, and studies have shown it to be particularly protective from redox agent-induced apoptosis [19]. HtrA2 was identified as notably upregulated ($p < 0.01$) by inference testing, although it was only 1.4-fold upregulated and thus not listed in Fig. 2. As with cytochrome *c*, HtrA2 is released from mitochondria in response to apoptotic stimuli, whereupon it inhibits the function of IAP (inhibitor of apoptosis) through direct binding, and may induce atypical cell death by a caspase-independent mechanism [20]. Finally, the upregulation of Anp32A and Anp32E may relate to the mitochondrial apoptotic pathway, and specifically the promotion of caspase-9 activation. Whilst Anp32 family members are well characterized as components of the SET complex controlling various aspects of mRNA stability, chromatin remodelling, and transcriptional regulation [21], Anp32A and Anp32E have also been shown to promote the activation of caspase-9 [22], the initiator caspase for the mitochondrial apoptotic pathway. The combined upregulation of reticulon 3, HtrA2, SAG, mtCLIC4, Anp32A, and Anp32E is consistent with active ER and mitochondrial apoptotic pathways, which is of particular interest given the profound hippocampal neuronal loss that occurs between 160 and 180 dpi, and our previous demonstration of apoptotic hippocampal CA1 pyramidal neurons within the ME7/CV scrapie model at 170 dpi [23].

ER stress is characterized by induction of the ER unfolded protein response (UPR) and ER overload response (EOR). Reticulon 3, discussed above in the context of ER stress, has recently been linked specifically to the EOR pathway [16]. Classical indicators of the UPR (e.g., glucose-regulated proteins (Grp)-58, -78, and -94, all previously associated with prion-mediated neurotoxicity [24]) were not identified as upregulated in the present study. However, several other ER-associated genes including chaperones and mediators of glycosylation were upregulated within the scrapie-infected hippocampus, either greater than 1.5-fold ($p < 0.01$) and thus listed in Fig. 2, or deemed of note by Empirical Bayes moderated *t* test but less than 1.5-fold (and thus not listed in Fig. 2). These include stromal cell-derived factor 2 [25] and β-1,3-*N*-acetylglucosaminyltransferase 1 [26], both of which are involved in glycosylation, and the ER chaperones FK506 binding protein 2 [27], Erp29 [28], and calnexin. Calnexin, which is a major ER chaperone responsible for folding of N-glycosylated proteins, is known to participate in the folding of PrP^C [29]. There is also significant upregulation of a cluster of genes involved in protein degradation, both through the ubiquitin–proteasome pathway (proteasome subunit β5 and ring finger proteins with ubiquitin E3 ligase activity) and through the lysosomal pathway (α-mannosidase 2 and ATPase, H^+ transporting V1 subunit D). α-Mannosidase 2 is involved specifically in the lysosomal turnover of glycoproteins. Various components of protein trafficking pathways are also upregulated, including signal recognition particle (SRP) 9, a component of the SRP complex which mediates recognition of secretory proteins and their targeting to the ER [30], the Golgi-localized short coiled-coil protein (Scoco) which is involved in regulating Golgi membrane traffic [31], and VAMP4 and AP1s1, both of which are involved in trafficking within the TGN-endosomal system [32]. This apparent upregulation of ER-resident chaperones and components of protein trafficking and degradation pathways is consistent with cells undergoing ER stress.

Several genes involved in cholesterol and lipid biosynthesis and metabolism were upregulated, including sterol-C5-desaturase, sterol-C4-methyl oxidase, acetyl-coenzymeA acyltransferase 1 (ACAT1; involved in cholesterol ester formation [33]), and sortilin-related receptor (a member of the low density lipoprotein (LDL)-receptor family involved in cholesterol transport [34]). Other cholesterol-related genes were also identified as notably upregulated by the Empirical Bayes moderated *t* test, albeit less than 1.5-fold. These include lecithin cholesterol acyltransferase (LCAT), involved in production of cholesterol esters [35], and very low-density lipoprotein receptor (VLDLR). Cholesterol esters become part of the lipid core of lipoproteins such as VLDL, thus upregulation of VLDLR may be a response to the increase in cholesterol esters brought about through the combined upregulation of ACAT1 and LCAT. Together, these observations are strongly suggestive of increased cholesterol biosynthesis within the preclinical ME7-infected hippocampus. This observation of upregulated cholesterol biosynthesis genes is consistent with the recent report of sterol-C4-methyl oxidase upregulation in ScN2A cells [36]. Timecourse QRT-PCR analysis of sterol-C4-methyl oxidase and sterol-C5-desaturase confirmed significant upregulation of these genes relative to uninfected controls at 170 dpi. Both genes are involved in the post-squalene phase of cholesterol biosynthesis, suggesting that their upregulation may be the cellular response to squalene accumulation, favouring its conversion to cholesterol. Whilst sterol-C4-methyl oxidase and sterol-C5-desaturase remained significantly upregulated at 180 and 210 dpi, a late-stage decline in expression of both genes occurred such that, by terminal disease, expression levels were at least comparable to the uninfected controls, if not marginally downregulated (Fig. 3). This is in agreement with another recent report describing downregulation of a cluster of genes involved in cholesterol biosynthesis at the terminal stage of disease [10]. The same pattern of early upregulation followed by terminal decline was identified for the neurofilament-L gene (Fig. 3), again consistent with a previous report of neurofilament-M and neurofilament-H downregulation at terminal disease [10]. It has previously been suggested that this downregulation of neuronal genes at terminal disease may reflect the loss of neuronal tissue [10]. However, the profound loss of hippocampal CA1 neurons occurs between 160 and 180 dpi in the ME7/CV model, after which the rate of further neuronal loss within the hippocampus is similar to that in age-matched controls [6]. Therefore, the detection of neuronal gene downregulation within the terminal-stage hippocampus relative to matched controls cannot be attributable simply to terminal neuronal loss. Whilst the terminal stage decrease in cholesterol biosynthesis-related gene expression has been reported previously, the earlier upregulation of these genes detected in the present study is a novel finding.

The final major functional group of significantly upregulated genes is that of transcription factors and gene products associated with chromatin architecture. At least 16 of the 65 upregulated genes identified in the present study are involved in some form of transcriptional control, although the significance of their upregulation is unclear as the group includes both co-activators and co-repressors of transcription. The transcription factors C/EBP δ (an important regulator of immune and inflammatory genes) and the interferon consensus sequence binding protein (ICSBP; involved in the activation of IFN-responsive genes), both previously reported as upregulated in scrapie-infected brain [10,11], were not detected in the present study. This is again consistent with the immune and inflammatory response to prion infection being at an early stage.

Thirteen genes were downregulated greater than 1.5-fold within the ME7-infected hippocampus, although these did not cluster into functionally assigned groups. Claudin 5, a structural molecule that is integral to tight junctions, was downregulated. Claudin 11 was similarly downregulated, although this did not meet the criteria for inclusion in Fig. 2. Their downregulation may reflect changes to the blood–brain barrier (BBB), as loss of tight junctions is a prominent feature of disease-related BBB disruption [37].

Discussion

Through the application of high-density oligonucleotide probe arrays to the study of gene expression within the preclinical ME7-infected hippocampus, we report the identification of 78 differentially expressed genes that include those indicative of ongoing cellular stress (oxidative stress response and ER-associated stress), activation of both the ER and mitochondrial apoptotic pathways, and an activated cholesterol biosynthesis pathway. These findings are of importance in dissecting the molecular mechanisms that underlie prion neurotoxicity in vivo.

To put the results of this study into context with other microarray and non-microarray studies of differential gene expression in TSE brain, the vast majority (approximately 95%) of the differentially expressed genes identified in the present study have not been previously associated with TSE molecular neuropathology. Whilst this may, in part, be due to the focus on the hippocampal brain region rather than whole brain analysis, it is likely that it is primarily a consequence of the time-point chosen (170 dpi), which was approximately 4 weeks prior to clinical disease and over 8 weeks prior to terminal disease. Generally, those genes that have been frequently associated with terminal stage TSE-infected brain were not significantly upregulated in the hippocampus of the ME7/CV scrapie model by 170 dpi. However, there were exceptions to this. Some genes previously associated with TSE neuropathology at the terminal stages of disease were significantly upregulated in the present study (as determined by Empirical Bayes moderated t test), albeit less than the stringent 1.5-fold change ($p < 0.01$) used as our criteria for inclusion in Fig. 2. For example, metallothionein II, cathepsin B, and scrapie-responsive gene 1 were all upregulated 1.3- to 1.4-fold ($p < 0.02$) in the present study. These low but significant changes confirm the array analysis can identify genes known to be changed in the disease process, and importantly confirm that the changes in gene expression observed in this study precede those associated with terminal disease. Similarly, markers of glial cell activation were not significantly upregulated in the present study. GFAP was upregulated only 1.4-fold ($p = 0.03$, Empirical Bayes moderated t test), whilst microglial activation markers Mac-1 (CD11b) and F4/80, both of which are significantly upregulated in the terminal stage ME7-infected hippocampus [23], were not detected in the present study in either control or ME7-infected samples. This is consistent with our aim of examining disease-associated gene expression unobscured by the late stage glial response.

It is well documented that the neuronal loss observed in TSEs is mediated, at least in part, by apoptosis [23,24,38–42]. The caspase-dependent apoptotic cascade can be initiated via cell surface receptors, mitochondrial stress or by ER stress. Several studies have demonstrated the involvement of a particular pathway in the apoptotic response to prion infection. Thus, the upregulation of FAS in 87V scrapie [38] and caspase-8 activation in PrP106–126-challenged neurons [43] suggests involvement of the extrinsic apoptotic pathway mediated by cell surface receptors, whilst activated caspase-12 in vitro and in vivo implicates the ER apoptotic pathway [24]. Indeed, the ER-dependent apoptotic pathway has been implicated in a range of neurodegenerative diseases characterized by misfolding and accumulation of proteins (for review, see [44]). However, it is important to note that whilst the stimulus for initiation of apoptosis may vary, significant interplay exists between the organelle-specific stress and apoptosis pathways. The upregulation of mediators of both ER- and mitochondrial-induced apoptosis observed in the present study is consistent with the well-documented mitochondrial involvement in ER stress-induced apoptosis (for review, see [45]).

The present study provides evidence of perturbed ER function, with upregulation of glycosylation enzymes, chaperones and protein trafficking, and degradation machinery. How the ER stress–response is activated in prion diseases, and indeed in other neurodegenerative conditions, remains uncertain. Generally, ER stress can be induced by disrupted calcium homeostasis or by the accumulation of misfolded proteins in the ER. However the calcium-dependence of ER chaperones means that disrupted calcium homeostasis can itself result in the accumulation of misfolded protein and the induction of the UPR (for review, see [46]). Some PrP mutants associated with familial prion diseases are retained in the ER [47,48], and stimulation of retrograde transport towards the ER has been shown to increase PrP^{Sc} accumulation [49]. Despite this evidence of ER involvement in prion disease pathogenesis, no PrP^{Sc} accumulation in the ER has been described in either sporadic or infectious forms of disease. It is perhaps more likely that any PrP^{Sc}-induced ER stress is mediated by altered calcium homeostasis rather than a direct accumulation of misfolded PrP in the ER. Indeed, a recent report that PrP^{C} limits calcium release from the ER and calcium uptake by the mitochondria [50] may suggest that loss of function of PrP^{C} during disease progression may partly contribute to the shift towards ER stress.

The demonstration of activated cholesterol biosynthesis genes within the ME7-infected hippocampus is a novel finding. Interestingly, recent studies have demonstrated a close association between cholesterol biosynthesis and the ER stress-associated UPR. However, it is unclear whether activated cholesterol biosynthesis is causative of ER stress, mediated by cholesterol-induced depletion of ER calcium stores [51,52], or whether it occurs as a consequence of ER stress through the aberrant proteolytic activation of the ER membrane bound sterol regulatory element binding proteins [53]. The activated cholesterol biosynthesis pathway observed in the present study is of interest given recent observations in Alzheimer's disease (AD) and in vitro studies of prion disease. Hypercholesterolemia has been shown to influence amyloid precursor protein processing [54], and altered cholesterol metabolism has been reported in the AD brain [55]. Treatment of neuronal cultures with cholesterol-lowering drugs reduces intracellular and extracellular levels of disease-associated Aβ peptides [56]. Similarly, in vitro studies of prion disease have demonstrated that depletion of cellular cholesterol reduces the conversion of PrP^{C} to PrP^{Sc} [57]. Whilst this has been attributed to the loss of cholesterol-dependent lipid rafts and the resulting disruption to raft-dependent cellular trafficking, the current observation that cholesterol biosynthesis is actually activated in response to prion infection may suggest another level of involvement for cholesterol, and/or its metabolites, in TSE neuropathology. Furthermore, the observation that the two most upregulated cholesterol-associated genes within the present study, sterol-C4-methyl oxidase and sterol-C5-desaturase, are involved in the post-squalene phase of cholesterol biosynthesis and may reflect squalene accumulation is intriguing, given that squalestatin, a specific inhibitor of squalene synthase, prevents PrP^{Sc} accumulation and protects neurons from prion neurotoxicity [58].

In conclusion, we have identified the differential expression of 78 genes within the ME7-infected hippocampus, at a preclinical timepoint unobscured by the profound inflammatory response that is evident at later stages of disease. The gene array data reveal evidence of cellular stress (oxidative stress and ER stress), activated ER and mitochondrial apoptotic pathways, and activated cholesterol biosynthesis within the scrapie-infected hippocampus. It is considered likely that these pathways contribute directly to the previously reported profound neuronal loss that occurs within the ME7-infected hippocampus at this timepoint. The precise mechanism by which these pathways become activated remains enigmatic, although, as in previous studies of prion disease neurodegeneration, altered calcium homeostasis is a central event in many of the pathways identified. This study provides valuable insight into the molecular mechanisms that underlie prion disease neuropathology in vivo, and highlight potential targets for therapeutic intervention.

Acknowledgment

This work was supported by a grant from the United Kingdom Biotechnology and Biological Sciences Research Council.

Appendix A. Supplementary data

Supplementary data associated with this article can be found, in the online version, at doi:10.1016/j.bbrc.2005.06.060.

References

[1] S.B. Prusiner, Prions, Proc. Natl. Acad. Sci. USA 95 (1998) 13363–13383.

[2] G.G. Kovacs, O. Kalev, H. Budka, Contribution of neuropathology to the understanding of human prion disease, Folia Neuropathol. 42 (Suppl. A) (2004) 69–76.

[3] A.E. Williams, L.J. Lawson, V.H. Perry, H. Fraser, Characterization of the microglial response in murine scrapie, Neuropathol. Appl. Neurobiol. 20 (1994) 47–55.

[4] J. Schultz, A. Schwarz, S. Neidhold, M. Burwinkel, C. Riemer, D. Simon, M. Kopf, M. Otto, M. Baier, Role of interleukin-1 in prion disease-associated astrocyte activation, Am. J. Pathol. 165 (2004) 671–678.

[5] M. Jeffrey, W.G. Halliday, J. Bell, A.R. Johnston, N.K. MacLeod, C. Ingham, A.R. Sayers, D.A. Brown, J.R. Fraser, Synapse loss associated with abnormal PrP precedes neuronal degeneration in the scrapie-infected murine hippocampus, Neuropathol. Appl. Neurobiol. 26 (2000) 41–54.

[6] M. Jeffrey, S. Martin, J. Barr, A. Chong, J.R. Fraser, Onset of accumulation of PrPRes in murine ME7 scrapie in relation to pathological and PrP immunohistochemical changes, J. Comp. Pathol. 124 (2001) 20–28.

[7] A.R. Johnston, J.R. Fraser, M. Jeffrey, N.K. MacLeod, Synaptic plasticity in the CA1 area of the hippocampus of scrapie-infected mice, Neurobiol. Dis. 5 (1998) 188–195.

[8] A.R. Brown, J. Webb, S. Rebus, A. Williams, J.K. Fazakerley, Identification of upregulated genes by array analysis in scrapie-infected mouse brains, Neuropathol. Appl. Neurobiol. 30 (2004) 555–567.

[9] R.C. Gentleman, V.J. Carey, D.M. Bates, B. Bolstad, M. Dettling, S. Dudoit, B. Ellis, L. Gautier, Y. Ge, J. Gentry, K. Hornik, T. Hothorn, W. Huber, S. Iacus, R. Irizarry, F. Leisch, C. Li, M. Maechler, A.J. Rossini, G. Sawitzki, C. Smith, G. Smyth, L. Tierney, J.Y. Yang, J. Zhang, Bioconductor: open software development for computational biology and bioinformatics, Genome Biol. 5 (2004) R80.

[10] C. Riemer, S. Neidhold, M. Burwinkel, A. Schwarz, J. Schultz, J. Kratzschmar, U. Monning, M. Baier, Gene expression profiling of scrapie-infected brain tissue, Biochem. Biophys. Res. Commun. 323 (2004) 556–564.

[11] W. Xiang, O. Windl, G. Wunsch, M. Dugas, A. Kohlmann, N. Dierkes, I.M. Westner, H.A. Kretzschmar, Identification of differentially expressed genes in scrapie-infected mouse brains by using global gene expression technology, J. Virol. 78 (2004) 11051–11060.

[12] J. Paloneva, T. Manninen, G. Christman, K. Hovanes, J. Mandelin, R. Adolfsson, M. Bianchin, T. Bird, R. Miranda, A. Salmaggi, L. Tranebjaerg, Y. Konttinen, L. Peltonen, Mutations in two genes encoding different subunits of a receptor signaling complex result in an identical disease phenotype, Am. J. Hum. Genet. 71 (2002) 656–662.

[13] K. Takahashi, C.D. Rochford, H. Neumann, Clearance of apoptotic neurons without inflammation by microglial triggering receptor expressed on myeloid cells-2, J. Exp. Med. 201 (2005) 647–657.

[14] M.K. Kwak, N. Wakabayashi, J.L. Greenlaw, M. Yamamoto, T.W. Kensler, Antioxidants enhance mammalian proteasome expression through the Keap1–Nrf2 signaling pathway, Mol. Cell. Biol. 23 (2003) 8786–8794.

[15] P. Dormer, E. Spitzer, W. Moller, EDR is a stress-related survival factor from stroma and other tissues acting on early haematopoietic progenitors (E-Mix), Cytokine 27 (2004) 47–57.

[16] E. Kuang, Q. Wan, X. Li, H. Xu, Q. Liu, Y. Qi, ER Ca(2+) depletion triggers apoptotic signals for endoplasmic reticulum (ER) overload response induced by overexpressed reticulon 3 (RTN3/HAP), J. Cell. Physiol. 204 (2005) 549–559.

[17] X. Qu, Y. Qi, P. Lan, Q. Li, The novel endoplasmic reticulum (ER)-targeted protein HAP induces cell apoptosis by the depletion of the ER Ca(2+) stores, FEBS Lett. 529 (2002) 325–331.

[18] E. Fernandez-Salas, K.S. Suh, V.V. Speransky, W.L. Bowers, J.M. Levy, T. Adams, K.R. Pathak, L.E. Edwards, D.D. Hayes, C. Cheng, A.C. Steven, W.C. Weinberg, S.H. Yuspa, mtCLIC/CLIC4, an organellular chloride channel protein, is increased by DNA damage and participates in the apoptotic response to p53, Mol. Cell. Biol. 22 (2002) 3610–3620.

[19] H. Duan, Y. Wang, M. Aviram, M. Swaroop, J.A. Loo, J. Bian, Y. Tian, T. Mueller, C.L. Bisgaier, Y. Sun, SAG, a novel zinc RING finger protein that protects cells from apoptosis induced by redox agents, Mol. Cell. Biol. 19 (1999) 3145–3155.
[20] Y. Suzuki, Y. Imai, H. Nakayama, K. Takahashi, K. Takio, R. Takahashi, A serine protease, HtrA2, is released from the mitochondria and interacts with XIAP, inducing cell death, Mol. Cell 8 (2001) 613–621.
[21] T.A. Santa-Coloma, Anp32e (Cpd1) and related protein phosphatase 2 inhibitors, Cerebellum 2 (2003) 310–320.
[22] X. Jiang, H.E. Kim, H. Shu, Y. Zhao, H. Zhang, J. Kofron, J. Donnelly, D. Burns, S.C. Ng, S. Rosenberg, X. Wang, Distinctive roles of PHAP proteins and prothymosin-alpha in a death regulatory pathway, Science 299 (2003) 223–226.
[23] A.R. Brown, J. Webb, S. Rebus, R. Walker, A. Williams, J.K. Fazakerley, Inducible cytokine gene expression in the brain in the ME7/CV mouse model of scrapie is highly restricted, is at a strikingly low level relative to the degree of gliosis and occurs only late in disease, J. Gen. Virol. 84 (2003) 2605–2611.
[24] C. Hetz, M. Russelakis-Carneiro, K. Maundrell, J. Castilla, C. Soto, Caspase-12 and endoplasmic reticulum stress mediate neurotoxicity of pathological prion protein, EMBO J. 22 (2003) 5435–5445.
[25] T. Hamada, K. Tashiro, H. Tada, J. Inazawa, M. Shirozu, K. Shibahara, T. Nakamura, N. Martina, T. Nakano, T. Honjo, Isolation and characterization of a novel secretory protein, stromal cell-derived factor-2 (SDF-2) using the signal sequence trap method, Gene 176 (1996) 211–214.
[26] D. Zhou, A. Dinter, G.R. Gutierrez, J.P. Kamerling, J.F. Vliegenthart, E.G. Berger, T. Hennet, A beta-1,3-*N*-acetylglucosaminyltransferase with with poly-*N*-acetyllactosamine synthase activity is structurally related to beta-1,3-galactosyltransferases, Proc. Natl. Acad. Sci. USA 96 (1999) 406–411.
[27] K.T. Bush, B.A. Hendrickson, S.K. Nigam, Induction of the FK506-binding protein, FKBP13, under conditions which misfold proteins in the endoplasmic reticulum, Biochem. J. 303 (1994) 705–708.
[28] D.M. Ferrari, V.P. Nguyen, H.D. Kratzin, H.D. Soling, ERp28, a human endoplasmic-reticulum-lumenal protein, is a member of the protein disulfide isomerase family but lacks a CXXC thioredoxin-box motif, Eur. J. Biochem. 255 (1998) 570–579.
[29] P.M. Rudd, M.R. Wormald, D.R. Wing, S.B. Prusiner, R.A. Dwek, Prion glycoprotein: structure, dynamics, and roles for the sugars, Biochemistry 40 (2001) 3759–3766.
[30] H.M. Dani, J. Singh, S. Singh, Advances in the structure and functions of signal recognition particle in protein targeting, J. Biol. Regul. Homeost. Agents 17 (2003) 303–307.
[31] H. Van Valkenburgh, J.F. Shern, J.D. Sharer, X. Zhu, R.A. Kahn, ADP-ribosylation factors (ARFs) and ARF-like 1 (ARL1) have both specific and shared effectors: characterizing ARL1-binding proteins, J. Biol. Chem. 276 (2001) 22826–22837.
[32] I. Hinners, F. Wendler, H. Fei, L. Thomas, G. Thomas, S.A. Tooze, AP-1 recruitment to VAMP4 is modulated by phosphorylation-dependent binding of PACS-1, EMBO Rep. 4 (2003) 1182–1189.
[33] P. Oelkers, A. Behari, D. Cromley, J.T. Billheimer, S.L. Sturley, Characterization of two human genes encoding acyl coenzyme A:cholesterol acyltransferase-related enzymes, J. Biol. Chem. 273 (1998) 26765–26771.
[34] L. Jacobsen, P. Madsen, C. Jacobsen, M.S. Nielsen, J. Gliemann, C.M. Petersen, Activation and functional characterization of the mosaic receptor SorLA/LR11, J. Biol. Chem. 276 (2001) 22788–22796.
[35] J.W. Furbee Jr., O. Francone, J.S. Parks, In vivo contribution of LCAT to apolipoprotein B lipoprotein cholesteryl esters in LDL receptor and apolipoprotein E knockout mice, J. Lipid Res. 43 (2002) 428–437.
[36] A.D. Greenwood, M. Horsch, A. Stengel, I. Vorberg, G. Lutzny, E. Maas, S. Schadler, V. Erfle, J. Beckers, H. Schatzl, C. Leib-Mosch, Cell line dependent RNA expression profiles of prion-infected mouse neuronal cells, J. Mol. Biol. 349 (2005) 487–500.
[37] J.D. Huber, R.D. Egleton, T.P. Davis, Molecular physiology and pathophysiology of tight junctions in the blood–brain barrier, Trends Neurosci. 24 (2001) 719–725.
[38] E. Jamieson, M. Jeffrey, J.W. Ironside, J.R. Fraser, Activation of Fas and caspase 3 precedes PrP accumulation in 87V scrapie, Neuroreport 12 (2001) 3567–3572.
[39] P.J. Lucassen, A. Williams, W.C. Chung, H. Fraser, Detection of apoptosis in murine scrapie, Neurosci. Lett. 198 (1995) 185–188.
[40] B. Puig, I. Ferrer, Cell death signaling in the cerebellum in Creutzfeldt–Jakob disease, Acta Neuropathol. (Berl) 102 (2001) 207–215.
[41] S. Siso, B. Puig, R. Varea, E. Vidal, C. Acin, M. Prinz, F. Montrasio, J. Badiola, A. Aguzzi, M. Pumarola, I. Ferrer, Abnormal synaptic protein expression and cell death in murine scrapie, Acta Neuropathol. (Berl) 103 (2002) 615–626.
[42] A. Williams, P.J. Lucassen, D. Ritchie, M. Bruce, PrP deposition, microglial activation and neuronal apoptosis in murine scrapie, Exp. Neurol. 144 (1997) 433–438.
[43] A.R. White, R. Guirguis, M.W. Brazier, M.F. Jobling, A.F. Hill, K. Beyreuther, C.J. Barrow, C.L. Masters, S.J. Collins, R. Cappai, Sublethal concentrations of prion peptide PrP106–126 or the amyloid beta peptide of Alzheimer's disease activates expression of proapoptotic markers in primary cortical neurons, Neurobiol. Dis. 8 (2001) 299–316.
[44] J. Castilla, C. Hetz, C. Soto, Molecular mechanisms of neurotoxicity of pathological prion protein, Curr. Mol. Med. 4 (2004) 397–403.
[45] D.G. Breckenridge, M. Germain, J.P. Mathai, M. Nguyen, G.C. Shore, Regulation of apoptosis by endoplasmic reticulum pathways, Oncogene 22 (2003) 8608–8618.
[46] W. Paschen, Dependence of vital cell function on endoplasmic reticulum calcium levels: implications for the mechanisms underlying neuronal cell injury in different pathological states, Cell Calcium 29 (2001) 1–11.
[47] T. Jin, Y. Gu, G. Zanusso, M. Sy, A. Kumar, M. Cohen, P. Gambetti, N. Singh, The chaperone protein BiP binds to a mutant prion protein and mediates its degradation by the proteasome, J. Biol. Chem. 275 (2000) 38699–38704.
[48] N. Singh, G. Zanusso, S.G. Chen, H. Fujioka, S. Richardson, P. Gambetti, R.B. Petersen, Prion protein aggregation reverted by low temperature in transfected cells carrying a prion protein gene mutation, J. Biol. Chem. 272 (1997) 28461–28470.
[49] F. Beranger, A. Mange, B. Goud, S. Lehmann, Stimulation of PrP(C) retrograde transport toward the endoplasmic reticulum increases accumulation of PrP(Sc) in prion-infected cells, J. Biol. Chem. 277 (2002) 38972–38977.
[50] M. Brini, M. Miuzzo, N. Pierobon, A. Negro, M.C. Sorgato, The prion protein and its paralogue Doppel affect calcium signaling in Chinese hamster ovary (CHO) cells, Mol. Biol. Cell (2005).
[51] B. Feng, P.M. Yao, Y. Li, C.M. Devlin, D. Zhang, H.P. Harding, M. Sweeney, J.X. Rong, G. Kuriakose, E.A. Fisher, A.R. Marks, D. Ron, I. Tabas, The endoplasmic reticulum is the site of cholesterol-induced cytotoxicity in macrophages, Nat. Cell Biol. 5 (2003) 781–792.
[52] Y. Li, M. Ge, L. Ciani, G. Kuriakose, E.J. Westover, M. Dura, D.F. Covey, J.H. Freed, F.R. Maxfield, J. Lytton, I. Tabas, Enrichment of endoplasmic reticulum with cholesterol inhibits sarcoplasmic–endoplasmic reticulum calcium ATPase-2b activity in parallel with increased order of membrane lipids: implications for depletion of endoplasmic reticulum calcium stores and apoptosis in cholesterol-loaded macrophages, J. Biol. Chem. 279 (2004) 37030–37039.

[53] J.N. Lee, J. Ye, Proteolytic activation of sterol regulatory element-binding protein induced by cellular stress through depletion of Insig-1, J. Biol. Chem. 279 (2004) 45257–45265.
[54] L.M. Refolo, M.A. Pappolla, B. Malester, J. LaFrancois, T. Bryant-Thomas, R. Wang, G.S. Tint, K. Sambamurti, K. Duff, Hypercholesterolemia accelerates the Alzheimer's amyloid pathology in a transgenic mouse model, Neurobiol. Dis. 7 (2000) 321–331.
[55] R.G. Cutler, J. Kelly, K. Storie, W.A. Pedersen, A. Tammara, K. Hatanpaa, J.C. Troncoso, M.P. Mattson, Involvement of oxidative stress-induced abnormalities in ceramide and cholesterol metabolism in brain aging and Alzheimer's disease, Proc. Natl. Acad. Sci. USA 101 (2004) 2070–2075.
[56] K. Fassbender, M. Simons, C. Bergmann, M. Stroick, D. Lutjohann, P. Keller, H. Runz, S. Kuhl, T. Bertsch, K. von Bergmann, M. Hennerici, K. Beyreuther, T. Hartmann, Simvastatin strongly reduces levels of Alzheimer's disease beta-amyloid peptides Abeta 42 and Abeta 40 in vitro and in vivo, Proc. Natl. Acad. Sci. USA 98 (2001) 5856–5861.
[57] A. Taraboulos, M. Scott, A. Semenov, D. Avrahami, L. Laszlo, S.B. Prusiner, Cholesterol depletion and modification of COOH-terminal targeting sequence of the prion protein inhibit formation of the scrapie isoform, J. Cell Biol. 129 (1995) 121–132.
[58] C. Bate, M. Salmona, L. Diomede, A. Williams, Squalestatin cures prion-infected neurones and protects against prion neurotoxicity, J. Biol. Chem. 279 (2004) 14983–14990.